

Manuscript Number:

Title: Limit analysis of W7-X critical magnet system components with consideration of material serration effect

Article Type: FUSION TECHNOLOGY 2010 SI

Keywords: cryogenic magnet system, finite element models, limit analysis, serration effect

Corresponding Author: Dr Łukasz Ciupiński,

Corresponding Author's Institution: Politechnika Warszawska

First Author: Łukasz Ciupiński

Order of Authors: Łukasz Ciupiński; Grzegorz Krzesiński, Ph.D.; Piotr Marek, Ph.D.; Tomasz Zagrajek, Prof.; Joris Fellingner, Ph.D.; Victor Bykov, Ph.D.; Andrzej Dudek, Ph.D.; Felix Schauer, Ph.D.; Anatoli Panin, Ph.D.

Abstract: The paper reports on finite element (FE) method analyses aiming at the determination of the static load bearing capacity of critical components in the support structure of superconducting coils of Wendelstein 7-X (W7-X). These components are made of austenitic stainless steel that at 4 K is known to exhibit instable plastic flow - the so called serration effect, i.e. a scattering of the stress under increasing strain. This material behavior may significantly reduce the load bearing capacity of the components. The developed modeling approach uses a special procedure to simulate the serration effect in a conservative way. The expected reduction of the material properties due to the welding process is also taken into account. It is demonstrated that the models are capable to determine the limit loads for the critical components in a flexible and efficient way.

Dear Sirs,

Herewith, I submit our paper entitled „ Limit analysis of W7-X critical magnet system components with consideration of material serration effect ”. Kindly please consider its publication in the special issue of the Fusion Engineering and Design journal. The extended abstract of the paper has been positively evaluated by the organizer of SOFT 2010 conference and we were invited to submit full manuscript.

With best regards,  
Łukasz Ciupiński

# Limit analysis of W7-X critical magnet system components with consideration of material serration effect

Łukasz Ciupiński<sup>a</sup>, Grzegorz Krzesiński<sup>a</sup>, Piotr Marek<sup>a</sup>, Tomasz Zagrajek<sup>a</sup>, Joris Fellingner<sup>b</sup>, Victor Bykov<sup>b</sup>, Andrzej Dudek<sup>b</sup>, Felix Schauer<sup>b</sup>, Anatoli Panin<sup>c</sup>

<sup>a</sup>Politechnika Warszawska, Pl. Politechniki 1, PL-00661 Warszawa

<sup>b</sup>Max-Planck-Institut für Plasmaphysik, Wendelsteinstraße 1, D-17491 Greifswald

<sup>c</sup>Forschungszentrum Jülich, Wilhelm-Johnen-Straße, D-52428 Jülich

The paper reports on finite element (FE) method analyses aiming at the determination of the static load bearing capacity of critical components in the support structure of superconducting coils of Wendelstein 7-X (W7-X). These components are made of austenitic stainless steel that at 4 K is known to exhibit instable plastic flow – the so-called serration effect, i.e. a scattering of the stress under increasing strain. This material behavior may significantly reduce the load bearing capacity of the components. The developed modeling approach uses a special procedure to simulate the serration effect in a conservative way. The expected reduction of the material properties due to the welding process is also taken into account. It is demonstrated that the models are capable to determine the limit loads for the critical components in a flexible and efficient way.

Keywords: cryogenic magnet system, finite element models, limit analysis, serration effect

## 1. Introduction

The magnetic field, confining the plasma of the W7-X experiment, is produced by a set of superconducting coils arranged in 5 identical modules with inverted symmetry between semi-modules [1]. Each coil is mounted on a central support structure (CSS) through two bolted connections called central support elements (CSEs). During operation, at a service temperature of 4K, the superconducting coils exert high forces and moments against each other, and against the CSS [2]. Therefore, detailed analyses of the CSEs are critical for the support structure [3]. The coil-side parts of the CSEs consist of extension blocks that are welded onto the coil cases. These welds are critical as far as the load bearing capacity of the structure is concerned. Both the coil cases and coil extension blocks are made of austenitic stainless steel designated EN 1.3960 (cast). At 4 K, this stainless steel is known to exhibit a serration effect, i.e. instability of plastic deformation as shown in Figure 1.

The phenomenon of instable plastic flow has been known for a long time and observed for many metallic materials tested at cryogenic temperatures [4]. Three specific features accompany this effect in austenitic stainless steel at 4K: audible acoustic emission, free-running plastic deformation, and heating in the deformation zone [5]. The serrated yielding observed in straining experiments has been explained by many authors in terms of changes in the character of moving dislocations from screw to edge [6, 7]. Seeger [6] pointed out that type of dislocations might change at very low temperatures because of lack of thermal energy necessary for generation and motion of dislocations of predominantly screw character. Also at 4K the excitation of the crystal lattice is very low and the edge dislocations move at lower stresses than the screw ones. Others,

following Basinski [4], take into account the low specific heat and thermal conductivity of stainless steel near absolute zero. They argue that the temperature rise due to heat generated by plastic deformation work could be significant in locally deformed regions, leading to drastic decrease of flow stress (negative slope of flow stress against temperature) [8]. Thus, a localized portion of the specimen will flow catastrophically under decreasing stress until the load is relaxed to a lower value, and then the material is cooled down again.

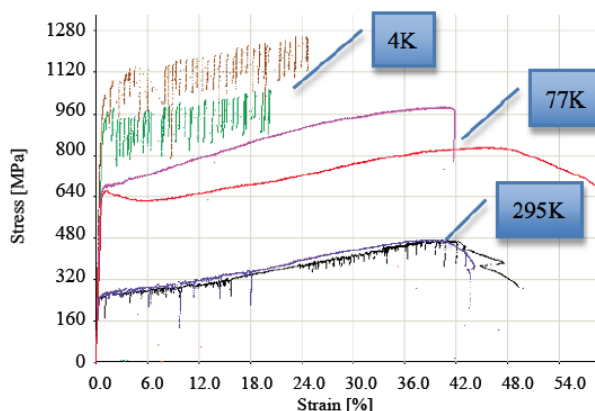


Fig. 1  $\sigma$ - $\epsilon$  relation of stainless steel 1.3960 at 295 K, 77K and 4K in a deformation controlled tensile test [material database W7-X]

It has been assumed in the present paper that regardless of the underlying phenomenon of the serration effect, it can have significant influence on the load bearing capacity of the material, thus possibly jeopardizing the structural stability of W7-X. Therefore, finite element (FE) models have been developed that enabled limit load analyses taking into account, in a conservative way, the material weakening due to the serration effect.

## 2. Modeling methodology

### 2.1 FE models

The FE models of all 14 different types of CSE extension blocks welded on the coils have been created in Ansys code [9] on the basis of CAD databases and technical drawings. All components were modeled with 3D solid elements, MPC 184 elements for load transfer and surface-to-surface contact elements if needed. The weld shape in each case was modeled in detail. The mesh density in the welds was determined in multiple test calculations of the first critical connection with varying meshes. Finally, the weld cross-section edges were divided into 4 to 6 solid elements. Special attention was also focused on the quality of the mesh in the neighborhood of the welds. Some simplifications concerning the shape of the coils and coil extension holes were made, but do not influence the results in the area of interest.

An exemplary FE model of the NPC1-Z1 connection as well as a close-up on the coil extension and the welds is shown in Fig. 2. A relevant part of the coil case was included in the FE model to avoid effects of the boundary conditions on the stress state near the weld between the blocks and the coil case. Fixed boundary conditions were applied at the cut edges of the coil case.

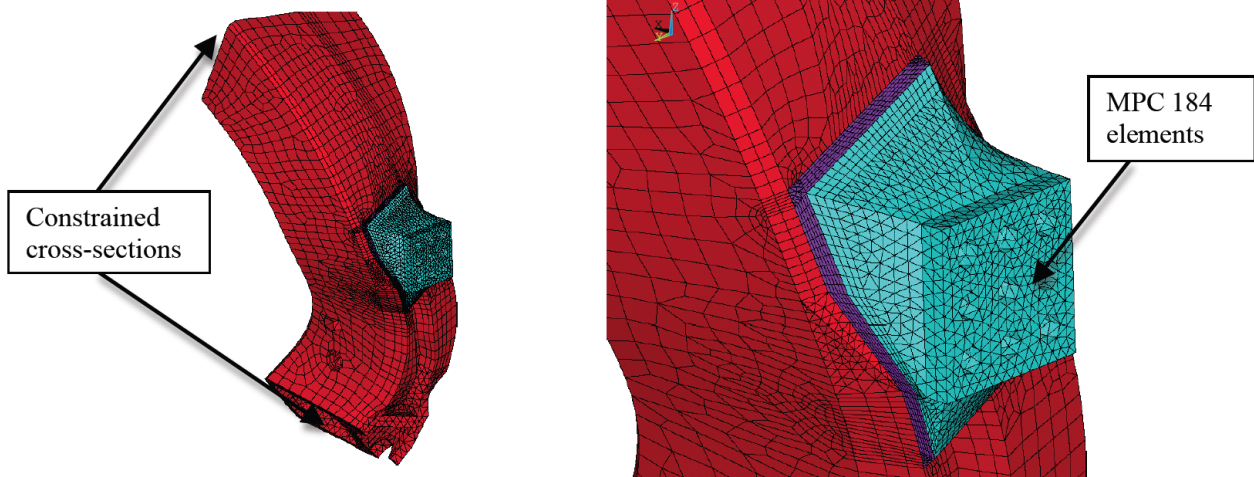


Fig. 2 FE model of NPC1-Z1 coil extension with detailed view on mesh density in weld vicinity

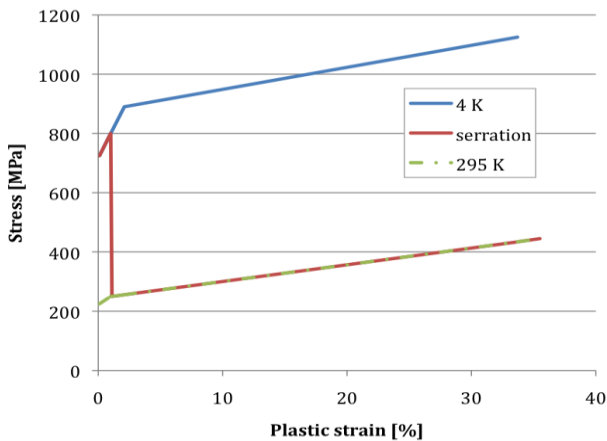


Fig. 3 Considered materials models (stress-plastic strain curves)

The design values of acting forces and moments were applied at the section through the coil extension block where the forces were extracted from the W7-X magnet system global model [3].

The models have been prepared as parametric ones. The adjustable macros enabled modifications of the following parameters: the material properties, weld efficiency factors, loads, convergence settings, load increment sizes, output data and output frequencies.

### 2.2 Material models

Four material models were implemented. Two of them described the material properties at 4 K and 295 K respectively and two others the serration effect (see Fig. 3). As a conservative estimate of the serration effect it was agreed that the material would respect the following behavior: (1) up to 1% of plastic strain the plastic hardening follows the yield curve as determined at 4 K, (2) beyond 1% of strain, as a consequence of the serration effect, it drops down and follows the yield curve as determined at 295 K.

This material behavior has been introduced into the ANSYS® database using two approaches: 1) a standard multi-linear stress-strain elasto-plastic curve with kinematic hardening (KINH) [9], 2) via a user defined

procedure for yield stress modification. For the latter the load was divided in multiple substeps. In each substep the plastic strains were calculated and automatically applied in the next substep as an artificial temperature field. The standard bi-linear kinematic hardening (BKIN) ANSYS material model was used to describe the material properties at different temperatures.

Both approaches for serration modeling were tested and checked at first using a simple FE tension test with one 3D element and then a 2D FE model of a rectangular plate with a circular hole under tension. The tests showed that both approaches of the serration modeling yield basically the same results, but the model with modified yield stress was generally more stable during the nonlinear calculations and less time consuming. The

conclusion was confirmed later by analyses of complex coil extensions.

### 2.3 Scope of analyses

The calculations have been performed for all 14 extension types. Either one or two load cases were selected for each extension from design ranges for nine plasma regimes at 3T operation. Two weld efficiency factors (0.85 and 1) were considered for each load case. Altogether, more than 160 model cases were analyzed.

The models were gradually loaded until failure with the static combination of forces and moments obtained from the W7-X global models. The calculations were run up to loss of convergence and in most cases the design load was exceeded. The failure was assessed and the load bearing capacity of the connection was estimated by monitoring agreed failure parameters.

### 3. Results

Although many calculations have been performed, only the most critical results are presented here. Table 1 summarizes the results of the selected analyses with serration effect and 0.85 weld efficiency factor.

In the table the values of the load ratios are given at which the agreed failure criteria were met. The load ratio is defined as a ratio of the current load applied to the design load (3 forces and 3 moments) as estimated from the W7-X global model.

The failure criteria labels presented in Table 1 denote:

- LAST: the last load at which the solution convergence was lost
- EPLA: equivalent von Mises plastic strain anywhere in the structure reaching 10% or 30% respectively
- Ku1: initial flexibility (for the first load step)
- Ku: tangent flexibility
- Kus: secant flexibility
- Ku/Ku1: relative tangent flexibility (1.5 and 2.5 respectively)
- Kus/Ku1: relative secant flexibility of 1.2 and 1.6 respectively
- PLAST: the percent of the total weld volume plastically deformed (25% and 75%)

The behavior of the analyzed structures is strongly nonlinear (see Fig.4, Fig.5) but corresponds well to the assumed models proving the reliability of the developed approach.

The relations between the limit loads obtained using different criteria depend on the considered case (the connection, the material model, the load case). The results show that, in most cases, the limit loads are greater than the design load with factor more than 1.5, which was chosen as criterion similar to limit analysis of warm structures [10]. When serration is considered and the weld efficiency factor is less than 1, for four extension types the calculation diverges already with a load factor below 1.5, and for NPC2z2 just factor 1.05 is reached (see Fig. 6). For three extension types some of prescribed criteria are violated before the models are loaded with the full design load.

### 4. Conclusions and further considerations

In the course of exploiting the operational limits of the machine, the objective of this task was to determine the static load bearing capacity of critical central support coil extension welds of W7-X taking into account, in a conservative way, the serration effect.

FE models that have been developed enabled limit load analyses for two different weld efficiency factors and used two different approaches for serration effect modeling. Results were also obtained for two extreme cases neglecting the serration effect, i.e. the models with 4K and RT material properties. The limit loads were estimated by predefined criteria including maximum plastic strain, the relative stiffness/flexibility of the connection, and the amount of plastified weld material.

The behavior of the models is strongly nonlinear. The response of the analyzed structures including the serration effects is very complex, but the failure mechanism is understandable and corresponds well to the applied load case and geometry of the connection. Both approaches for modeling serration effect yield very similar results, but the developed technique with artificial temperature fields leads to a better convergence of the solution process and can be recommended for such applications.

The estimated limit load ratios were the highest for the 4K material models and the lowest for the 295K ones, with the serration material models in between those two. The analyses allowed identification of the most critical connections. Taking into account the very conservative assumptions one cannot conclude from these results that some extreme W7-X field configuration might not be reached or operation could otherwise be restricted. Nevertheless, special attention shall be given to these connections. Undoubtedly, these findings

Table 1: Critical load ratios for selected connections - models with serration effect and 0.85 weld efficiency factor

	Load case	LAST	EPLA		Ku/Ku1		Kus/Ku1		PLAST	
			10	30	1.5	2.5	1.2	1.6	25	75
NPC1-Z1	L1	1.73	1.565	1.725	1.555	1.565	1.61	1.71	1.56	1.625
	L2	1.74	1.495	1.7	1.48	1.491	1.525	1.695	1.51	1.605
NPC2-Z2	L1	1.08	0.93	1.075	0.9	0.905	0.95	1.045	1.04	1.08
	L2	1.08	0.93	1.075	0.9	0.905	0.95	1.045	1.04	1.08
PCA-Z1	L1	2.57	2.54	-	2.3	2.52	2.56	-	2.075	2.4
	L2	2.57	2.54	-	2.3	2.52	2.56	-	2.075	2.4
PCA-Z2	L1	4.55	2.9	4.45	3.8	4.07	4.3	4.45	3.25	3.9
	L2	5.3	3.5	4.55	4.35	4.46	4.55	4.85	3.35	4

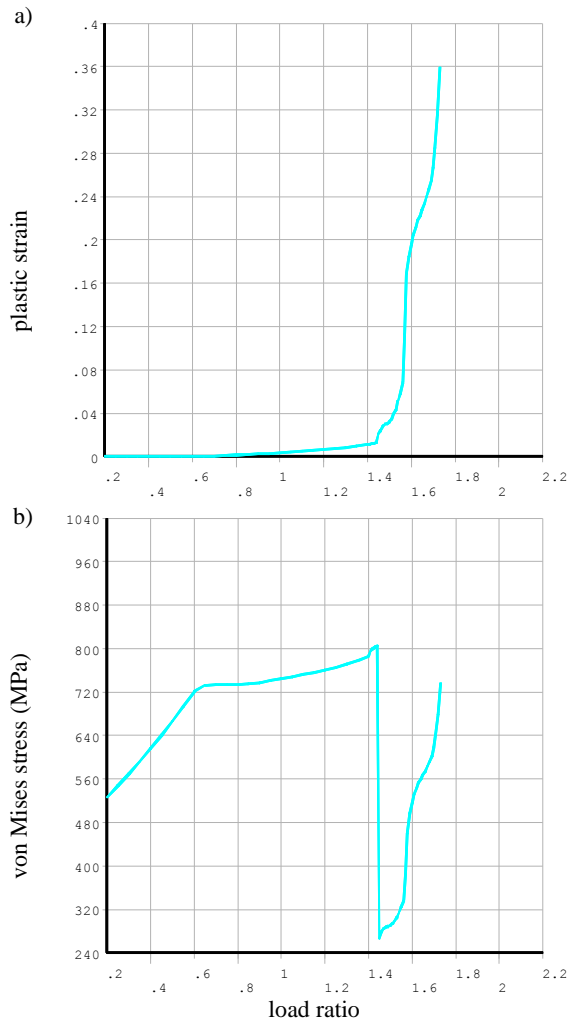


Fig. 4 NPC1-Z1. Load 1. (a) The maximum plastic strain vs. load ratio and (b) corresponding von Mises stress (MPa)

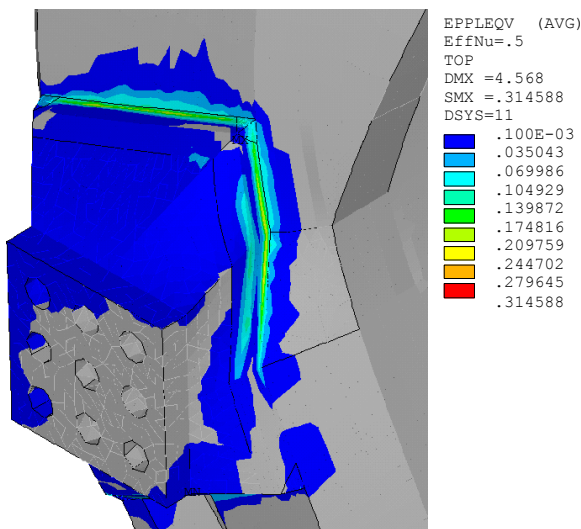


Fig. 5 NPC1-Z1. Load 1. Equivalent plastic strain distribution corresponding to the final load (load ratio 1.73)

prove the viability of the developed method for the assessment of the structural safety of the machine.

Two approaches are under consideration now for the critical coil extensions in order to verify that all 3 T field configurations can be completely reached: 1) less

conservative serration effect with a drop to the 77 K curve instead of the RT one. The assumption looks reasonable after a more detailed survey of literature, test results, and coupled thermal mechanical analyses for the W7-X loading speed; 2) introduction of the developed local models into the GM in order to realize more realistic boundary conditions for the extensions.

## Acknowledgments

This work has been a part of the EURATOM-IPPLM Physics Program funded by European Communities and Polish Ministry for Science and Higher Education under the contracts nos FU07-CT-2007-00061 and 1170/7PR-EURATOM/2009/7, respectively.

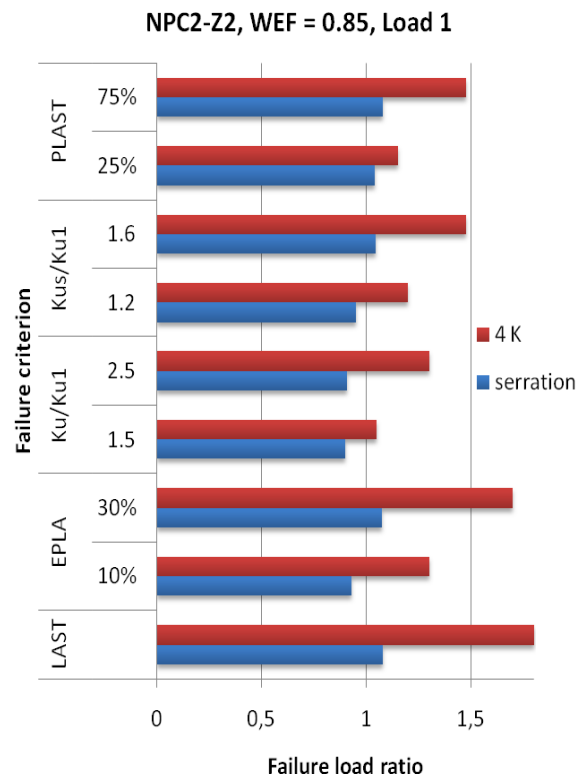


Fig. 6 NPC2-Z2. Comparison of the critical load ratios for models with 4K and serration materials properties

## References

- [1] M. Wanner et al., Fusion Eng. Des. 56–57, 155–162 (2001)
- [2] G. Krzesiński et al., Fusion Eng. Des. 82, 1574–1578 (2007)
- [3] V. Bykov et al., Fusion Eng. Des. 84, 215–219 (2009)
- [4] Z. S. Basinski, Proceedings of the Royal Society of London, Series A, Vol. 240, No. 1221 (1957), 229–242
- [5] R.L. Tobler, et al., Cryogenics 37, 533–550 (1997)
- [6] A. Seeger, Dislocations and Mechanical Properties of Crystals, p. 243, John Wiley & Sons, New York, 1957
- [7] B. Obst et al., Materials Sci. Eng. A137, 141–150 (1991)
- [8] R.P. Reed et al., Adv Cryogenic Eng 36B, 1077–1086 (1990)
- [9] ANSYS Release 11.0 Documentation, Ansys Inc., Houston, USA, 2007
- [10] ASME B&PV code, sec. VIII, Div. 2 (2001)

**Figure captions**

Fig. 7  $\sigma$ - $\epsilon$  relation of stainless steel 1.3960 at 295 K, 77K and 4K in a deformation controlled tensile test [material database W7-X]

Fig. 8 FE model of NPC1-Z1 coil extension with detailed view on mesh density in weld vicinity

Fig. 9 Considered materials models (stress-plastic strain curves)

Fig. 10 NPC1-Z1. Load 1. (a) The maximum plastic strain vs. load ratio and (b) corresponding von Mises stress (MPa)

Fig. 11 NPC1-Z1. Load 1. Equivalent plastic strain distribution corresponding to the final load (load ratio 1.73)

Fig. 12 NPC2-Z2. Comparison of the critical load ratios for models with 4K and serration materials properties

**Table captions**

Table 2: Critical load ratios for selected connections - models with serration effect and 0.85 weld efficiency factor

Table 1

	Load case	LAST	EPLA		Ku/Ku1		Kus/Ku1		PLAST	
			10	30	1.5	2.5	1.2	1.6	25	75
NPC1-Z1	L1	1.73	1.565	1.725	1.555	1.565	1.61	1.71	1.56	1.625
	L2	1.74	1.495	1.7	1.48	1.491	1.525	1.695	1.51	1.605
NPC3-Z1	L1	0.94	0.933	-	0.87	0.913	0.92	0.94	0.8	-
PCA-Z1	L1	2.57	2.54	-	2.3	2.52	2.56	-	2.075	2.4
PCA-Z2	L1	4.55	2.9	4.45	3.8	4.07	4.3	4.45	3.25	3.9
	L2	5.3	3.5	4.55	4.35	4.46	4.55	4.85	3.35	4



Figure 1

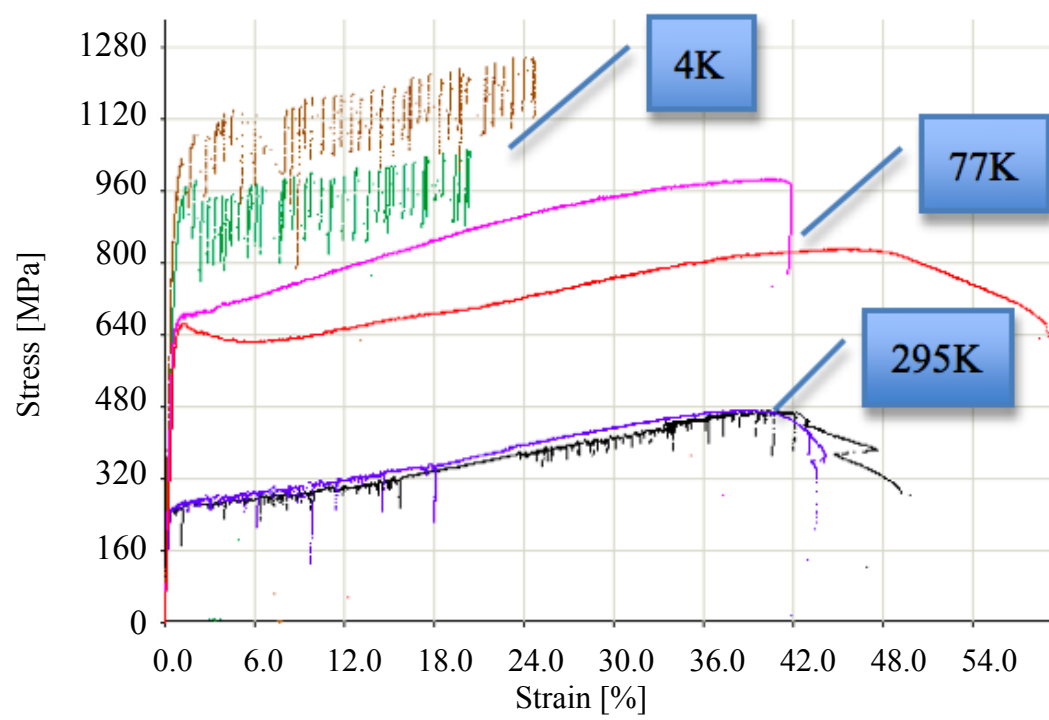


Figure 2

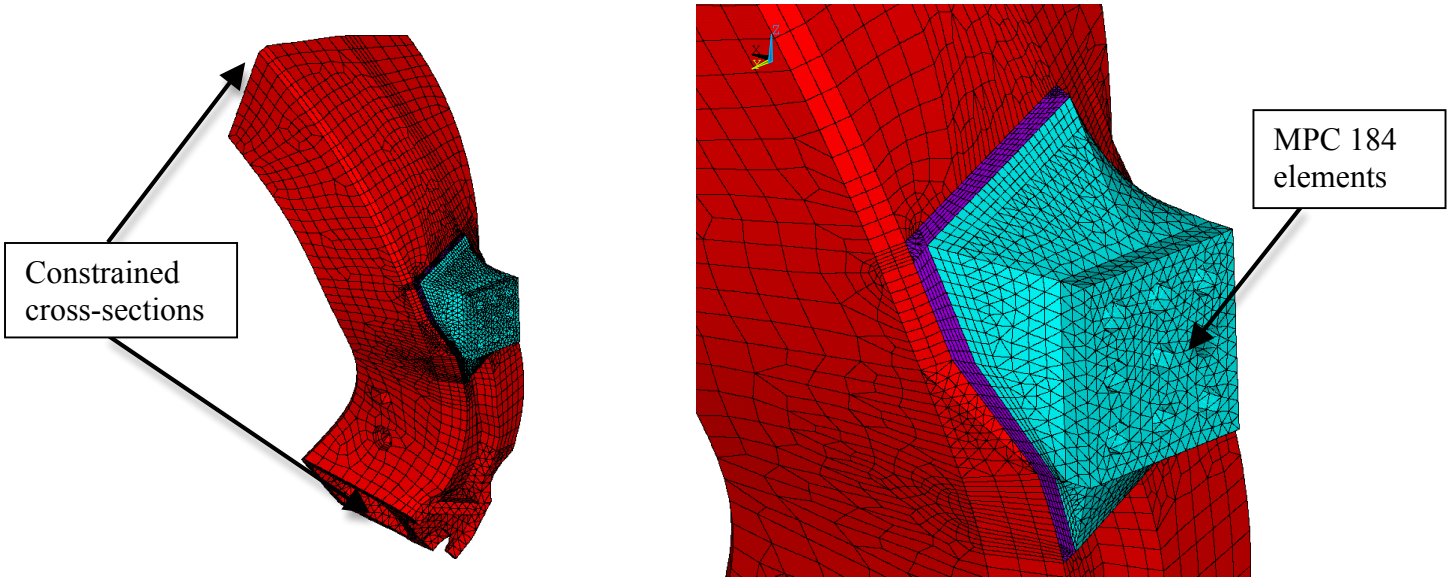


Figure 3

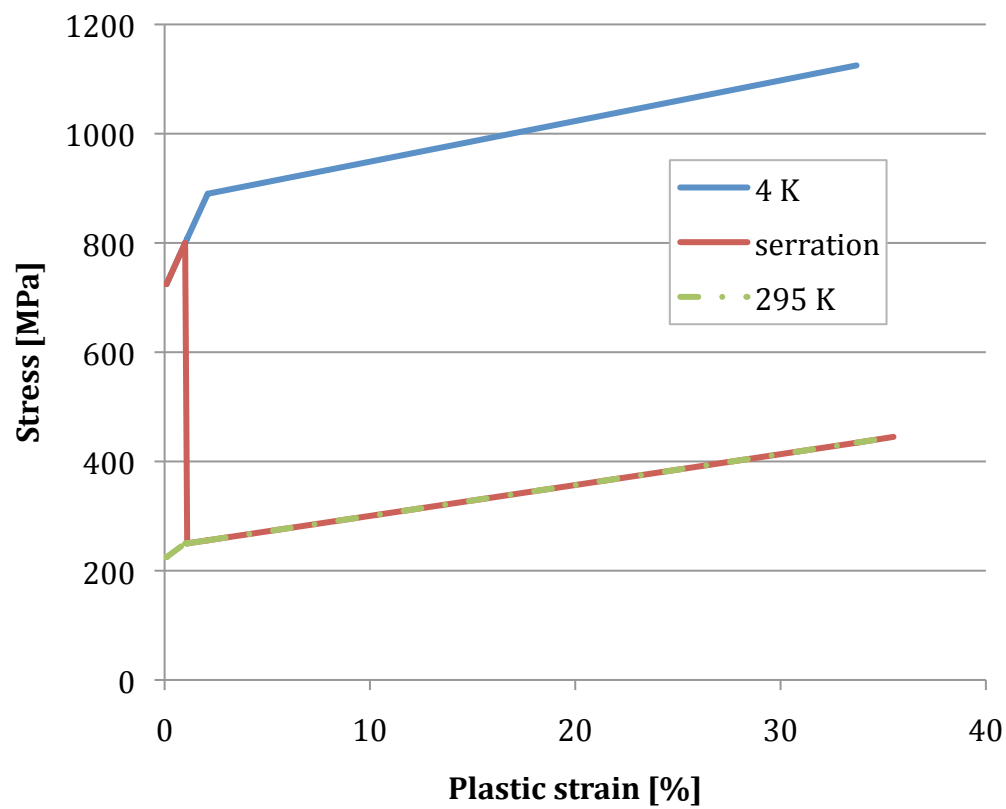


Figure 4

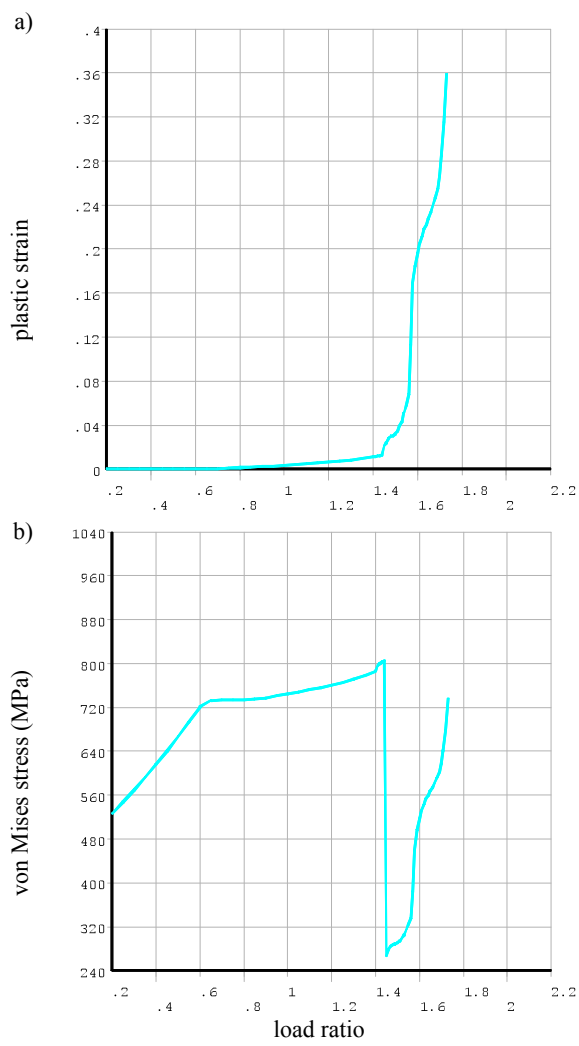


Figure 5

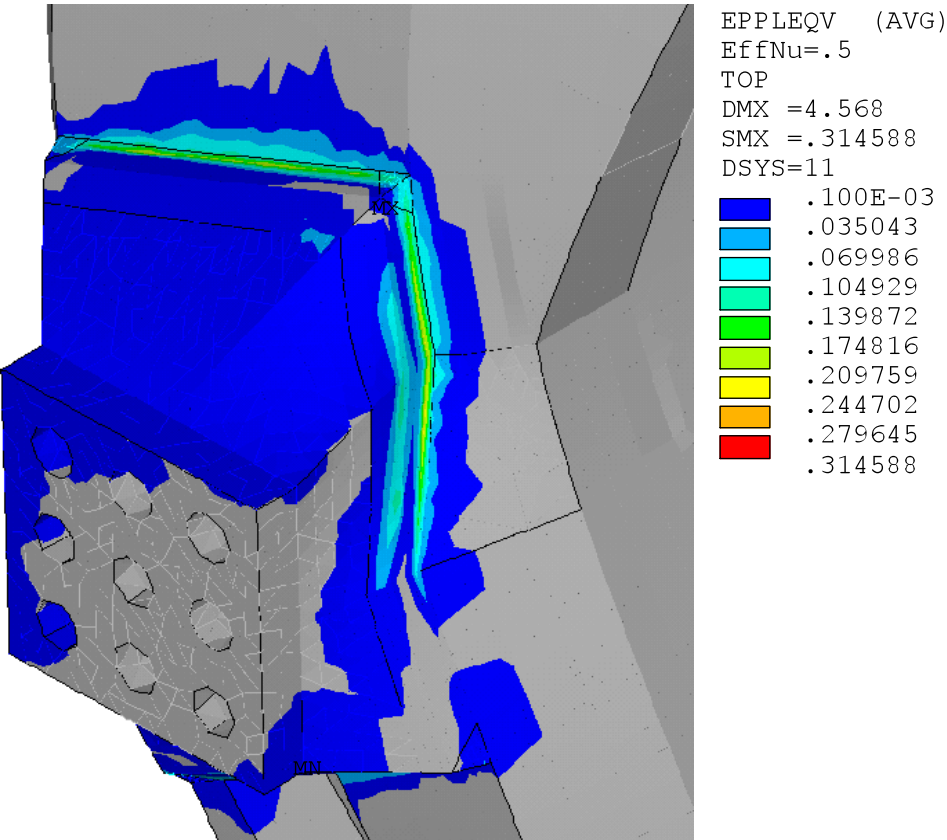


Figure 6

